

**The effects of oxygen plasma on the chemical composition and morphology of the Ru capping layer of the extreme ultraviolet (EUV) mask blanks**

***Leonid Belau<sup>1</sup>, Jeong Y. Park<sup>2</sup>, Ted Liang<sup>4</sup>, and Gabor A. Somorjai<sup>1,2,3\*</sup>***

*<sup>1</sup> Department of Chemistry, University of California, Berkeley, California 94720*

*<sup>2</sup> Chemical Sciences Division, Lawrence Berkeley National Laboratory, Berkeley, CA 94720*

*<sup>3</sup> Materials Sciences Division, Lawrence Berkeley National Laboratory, Berkeley, CA 94720*

*<sup>4</sup> Components Research, Technology and Manufacturing Group, Intel Corporation, Santa Clara, CA 95054*

**ABSTRACT**

Contamination removal from extreme ultraviolet (EUV) mask surfaces is one of the most important aspects to improve reliability for the next generation of EUV lithography. We report chemical and morphological changes of the ruthenium (Ru) mask surface after oxygen plasma treatment using surface sensitive analytical methods: X-ray photoelectron spectroscopy (XPS), atomic force microscopy (AFM) and transmission electron microscopy (TEM). Chemical analysis of the EUV masks shows an increase in the subsurface oxygen concentration, Ru oxidation and surface roughness. XPS spectra at various photoelectron takeoff angles suggest that the EUV mask surface was covered with chemisorbed oxygen after oxygen plasma treatment. It is proposed that the Kirkendall effect is the most plausible mechanism that explains the Ru surface oxidation. The etching rate of the Ru capping layer by oxygen plasma was estimated to be  $1.5 \pm 0.2$  Å/min, based on TEM cross sectional analysis.

\* Corresponding author, e-mail address: somorjai@berkeley.edu

## I. INTRODUCTION

One of the most promising methods for next generation semiconductor fabrication is extreme ultraviolet (EUV) lithography, operating at a wavelength of 13.5 nm. Special masks with reflective coatings and patterns that absorb EUV radiation are most frequently used for EUV lithography. The reflective coating of 30-50 Si/Mo multilayers is protected from oxidation by a 2.5 nm thick Ru capping layer that is deposited atop the Si layer.<sup>1</sup> One of the challenges of EUV lithography is to avoid any changes of the EUV mask and mirrors in an exposure tool during lithography or storage. Moreover, the demand for sub-30 nm patterning capability introduces new requirements in order to avoid contamination of the EUV mask surface with nano-particles.<sup>2</sup> Thus, cleaning and reflectivity restoration of the EUV mask is one of the most important processes during lithography.

Oxygen plasma is widely used for resist strip in semiconductor wafer processing. Additionally, among the many cleaning methods used in the semiconductor industry, O<sub>2</sub> plasma is known as an effective method for carbonaceous contamination removal without adding new particles on the surface.<sup>3,4</sup> However, oxygen plasma is known to etch Ru metal.<sup>5</sup> Removal of the Ru capping layer from the EUV reflecting coating reduces the durability of the EUV mask. Also oxygen plasma enhances the oxidation of the Ru capping layer. This significant amount of subsurface oxygen is incorporated into the Ru lattice that absorbs EUV radiation, reducing the reflectivity of the EUV mask.<sup>4,6,7</sup> It is, therefore, important to understand the mechanism of the corrosive gas phase-surface interactions to improve existing cleaning processes and Ru-based capping layer of the EUV mask. This is part of a broader effort in the investigation of surface changes of Ru-based capping layer in various cleaning chemistries under different conditions

Oxidation of Ru is a complex process; chemisorbed oxygen is found together with dissolved oxygen in the Ru lattice.<sup>8</sup> Core level X-ray photoelectron spectroscopy (XPS) is usually used to investigate chemical changes evolving near the surface in the Ru 3d and O 1s spectral regions. It was discovered that the most common oxide species during Ru surface treatment with oxygen plasma is RuO<sub>2</sub>. There is much speculation, however, about the probability of finding RuO<sub>3</sub> and RuO<sub>4</sub> on the surface. XPS spectra suggest that these volatile species do not remain on the surface.<sup>9</sup> Moreover, scanning tunneling microscopy (STM) studies suggest that surface Ru oxidation in an oxygen rich environment creates surface RuO<sub>2</sub> that coexists with metallic Ru covered by a chemisorbed oxygen monolayer O(1 × 1).<sup>10</sup>

In this paper, the effect of oxygen plasma cleaning on the chemical composition of the Ru capping layer is studied using surface sensitive spectroscopic and microscopic techniques: XPS, atomic force microscopy (AFM) and transmission electron microscopy (TEM).<sup>11</sup> XPS was utilized to study the change of the surface composition after surface treatment for both normal and grazing photoelectron takeoff angles. AFM was used to study changes of the surface morphology and roughness, confirming the occurrence of surface contamination during cleaning.

## II. EXPERIMENTAL DETAILS

An EUV mask is fabricated using magnetron sputter deposition of 40 multilayers (ML) of alternating Si and Mo with a standard period of 6.88 nm, on two 4" Si wafers. One mask is capped with a 3 nm Ru layer (close to the normal thickness currently employed for ML blanks) and other one with a 6 nm Ru layer (for purpose of easy characterization). For oxygen plasma cleaning, a PDC-32G (Harrick plasma) is utilized at full power of 18 W, equipped with a dry vacuum pump. The base pressure is 8 Pa (60 mTorr). The operating pressure flow during cleaning experiments is 67 Pa (500 mTorr).

Chemical surface composition is studied using high resolution NOVA XPS (Kratos) with an X-ray monochromator and an Al  $K_{\alpha}$  anode (operated at 1486.6 eV). Surface morphology analysis is performed using a Molecular Imaging AFM (RHK Technology), operated in contact mode using a silicon nitride tip (Budget sensor). The TEM images were taken with 200 KeV electrons on a JEOL 2010F field emission transmission electron microscope.

### III. RESULTS and DISCUSSIONS

The high resolution XPS spectra of the 6 nm Ru capping layer after 5 min of oxygen plasma treatment are shown in Figure 1, obtained at both normal and grazing photoelectron takeoff angles relative to the target surface,  $90^{\circ}$  and  $10^{\circ}$ , respectively. There are two major components that contribute to the shape of the photoelectron peak in the  $Ru3d_{5/2}$  region. The peak at the lower binding energy is attributed to the metallic Ru ( $Ru^0$ ) and the peak at the higher binding energy is due to the most stable oxide,  $RuO_2$  ( $Ru^{4+}$ ). Spectra comparison at the normal photoelectron takeoff angle in the  $Ru3d_{5/2}$  region, Figure 1(a), emphasizes the rises of the  $Ru^{4+}$  peak after oxygen plasma treatment. This suggests that the Ru capping layer is oxidized during the treatment. Moreover, it is interesting to note that the  $Ru^{4+}$  contribution to the overall peak shape in the  $Ru3d_{5/2}$  region is significantly larger in the XPS spectrum obtained at the grazing photoelectron takeoff angle, as shown in Figure 1(c). Due to the fact that surface sensitivity of the XPS measurement is highest at the grazing photoelectron takeoff angle, it is plausible to conclude that the concentration of  $RuO_2$  is higher near the surface of the EUV mask. The list of XPS peaks, assigned in the spectra of Figure 1, is tabulated in Table I.

Peak assignment in the  $Ru3d_{3/2}$  region is more ambiguous than in the  $Ru3d_{5/2}$  region due to the overlap of the C 1s and the Ru  $3d_{3/2}$  bands. However, the spectral broadening peak at the high binding energy side of the Ru  $3d_{3/2}$  is noticeable after oxygen plasma treatment at normal

and grazing photoelectron takeoff angles, Figures 1(a) and 1(c), respectively. One can notice that the Ru3d<sub>3/2</sub> peak relative intensity is larger than the Ru3d<sub>5/2</sub> peak at the grazing photoelectron takeoff angle. This is due to surface contamination with carbonaceous species being localized at the mask surface.

XPS spectra comparisons in the O 1s region, Figures 1(b) and 1(d), show that oxygen plasma substantially increases the oxygen concentration in Ru and support the conclusion that the Ru capping layer is oxidized during treatment. There are two distinguishable peaks responsible for the O 1s peak intensity rise in Figure 1(b): the peak at the lower binding energy is associated with oxygen atoms from RuO<sub>2</sub> (O<sup>2-</sup>) and the peak at the higher binding energy corresponds to weakly bounded oxygen atoms associated with chemisorbed and dissolved (subsurface) oxygen in the Ru lattice and on the surface.<sup>12</sup>

Figure 1(d) shows that the spectral pattern in the O 1s region at the grazing photoelectron takeoff angle does not distort after oxygen plasma treatment. In both spectra, before and after treatment (dashed and filled lines, respectively), the weakly bound oxygen is most abundant in the XPS spectrum. This fact suggests that chemisorbed oxygen, together with weakly bound subsurface oxygen, is the most abundant oxygen species near the surface of the Ru capping layer and that EUV mask treatment with reactive oxygen species does not change the Ru capping layer surface termination.

Based on the angular resolved XPS studies described above and previously reported experimental evidences of chemisorbed oxygen on Ru metal,<sup>10</sup> we propose a model to describe chemical changes of the Ru capping layer that evolve after oxygen plasma treatment. The model is based on the Kirkendall effect, which was proposed by Smigelkas and Kirkendall in 1947.<sup>13</sup> They found that the inter-diffusion of copper and zinc in brass is the result of the atomic

diffusion through vacancy exchange and not due to regular atoms diffusing. Recently Yin *et al.* postulated that oxidation of Fe and Co nanoparticles is taking place via the same effect<sup>14</sup>. One can assume that Ru oxidation by reactive oxygen radicals and ions from the plasma form RuO<sub>2</sub> in the vicinity of the mask surface, leading to the formation of defects and vacancies in the Ru lattice. Following the initial surface oxidation, Ru atoms from the bulk diffuse to the surface, creating a layer of metallic Ru which is instantly covered with chemisorbed oxygen. Thus, after oxygen plasma treatment, the mask surface is covered with unoxidized Ru atoms and chemisorbed oxygen, which is the dominant component in the O 1s region at the grazing photoelectron takeoff angle.

Comparison of the XPS spectra of the 6 nm and 3 nm Ru capping layers at two different photoelectron takeoff angles after oxygen plasma is shown in Figure 2. Spectra in Figure 2 are calibrated to the intensity of the Ru 3d<sub>5/2</sub> peak associated with RuO<sub>2</sub> (at 280.4 eV). XPS spectra comparisons in the Ru 3d<sub>5/2</sub> region at normal photoelectron takeoff angle, Figure 2(a), show that the relative intensity ratio of the Ru<sup>4+</sup>/Ru<sup>0</sup> peaks (oxidation ratio) is significantly higher in the case of the 3 nm Ru capping layer. A higher oxidation ratio for the thinner Ru layer is anticipated due to the same oxidation rate of Ru in both samples. This effect is pronounced when comparing spectra at the grazing photoelectron takeoff angle, Figure 2(c).

XPS spectra comparisons in the O 1s region suggest that the concentration of the weakly bound oxygen is significantly greater on the surface of the thinner (3 nm) Ru capping layer sample. XPS spectra in Figure 2(b) emphasize that the intensity of the weakly bounded oxygen peak around 531 eV is higher in the 3 nm than in the 6 nm Ru capping layer. This effect is more obvious in the spectra collected at the grazing photoelectron takeoff angle Figure 2(d). Since the amount of chemisorbed oxygen is the same for 3 nm and 6 nm films, it is plausible that the

concentration of the weakly bound oxygen is greater in the vicinity the mask surface capped with the thinner Ru layer. This effect is due to the higher O/Ru ratio, as achieved in the thinner film.

Surface morphology of the Ru capping layer undergoes significant changes after oxygen plasma treatment, as revealed by AFM analysis. The surface roughness increases gradually from  $2.2 \pm 0.4 \text{ \AA}$  to  $5.3 \pm 0.8 \text{ \AA}$ , corresponding to an untreated sample and after 4 min of oxygen plasma treatment, respectively. Figure 3 summarizes the AFM roughness measurements of the 3 nm Ru capping layer on the EUV mask.

The Ru capping layer etching is the most plausible explanation for the surface roughness increase after oxygen plasma treatment. The thickness change of the Ru capping layer after plasma treatment is studied using cross sectional TEM analysis. TEM micrographs before and after treatment are superimposed in such a way that the Si/Mo multilayer structure overlaps, as depicted in Figure 4(a) and 4(b). Black lines help to visualize the surface level in both micrographs. Superimposed micrographs reveal that the Ru capping layer shrinks by  $9 \pm 1 \text{ \AA}$  after the oxygen plasma treatment. This corresponds to an etching rate of  $1.5 \pm 0.2 \text{ \AA /min}$  of the Ru capping layer. It is important to say at this point that the etching rate is extremely sensitive to experimental conditions.

It was established experimentally that Ru etching by oxygen plasma is primarily due to the formation of volatile  $\text{RuO}_4$ , as this species was found in the gas phase during oxygen plasma treatment.<sup>5</sup> It is most likely that etching of the Ru capping layer from the EUV mask, even at moderate oxygen plasma conditions, is undertaken in a similar way by removal of the volatile  $\text{RuO}_4$  following Ru oxidation.

The reflectivity change of the EUV mask at a wavelength of 13.5 nm is an important reliability test for using oxygen plasma treatment to reduce contamination from the mask surface

in industrial applications. We measured the reflectivity of two masks, with a 3 nm or a 6 nm Ru capping layer, as a function of oxygen plasma exposure (up to 4 minutes). The reflectivity for masks with a 3 nm or a 6 nm Ru capping layer at a wavelength of 13.5 nm are 59.5 % and 52.0 %, respectively. We did not observe any significant decay of reflectivity values up to oxygen plasma exposure time of 4 minutes, which could be associated with two competing factors; increase of the EUV radiation losses caused by the high oxygen concentration and Ru etching. However, higher oxygen plasma doses result in removal of Ru layers and a higher oxygen concentration, therefore, leading to the failure mechanism of EUV masks. Our future work involves the study of chemical and morphological properties of the Ru capping after other advanced cleaning methods, including chemical cleaning process with acids, ozonated and hydrogenated waters, and exposure to ultraviolet light in the presence of oxygen.

Although the Ru capping layer provides some level of resistance to corrosion and oxidation during the EUV mask cleaning, it is not supplying complete protection of the underlying Si/Mo reflective coating. It has been demonstrated that the oxygen plasma treatment of the Ru capping layer does not form a passivation oxide layer on the surface, as in silver or palladium oxidation.<sup>15</sup> Thus we suggest that modification of the existing capping layer on the EUV mask in order to minimize the effect of oxygen dissolution. One of the possible solutions could be utilization of a bimetallic capping layer, RuX, that might reduce the number of vacancies in the Ru lattice and make the film amorphous.

#### **IV. CONCLUSIONS**

In this paper, we summarize studies showing changes in chemical and physical properties of the Ru capping layer after oxygen plasma treatment. These study use XPS, AFM and TEM and reflectivity measurements. XPS studies of the EUV mask in the Ru 3d and O 1s regions



emphasize that although oxygen plasma treatment removes organic contamination, the subsurface oxygen concentration substantially increases, as does Ru oxidation. It was shown that RuO<sub>2</sub> is formed near the surface after oxygen plasma treatment. Angular resolved XPS analysis suggests that chemisorbed oxygen on metallic Ru atoms together with subsurface oxygen are the most common sources of oxygen on the Ru capping layer surface, even after extensive Ru oxidation. Based on these considerations, it is proposed that the Kirkendall effect is the most plausible model describing the Ru capping layer oxidation: bulk Ru atoms diffuse to the surface through available vacancies in the lattice following oxidation of the Ru atoms near the surface. EUV mask treatment with oxygen plasma increases surface roughness due to Ru etching, as revealed from AFM measurements. However, the etching rate of the Ru capping layer is very dependent on experimental conditions. The etching rate of  $1.5 \pm 0.2$  Å/min of the Ru capping layer has been experimentally determined, comparing the high resolution TEM micrographs before and after oxygen plasma treatment. Reflectivity measurements show that oxygen plasma treatment does not change the reflectivity properties of the EUV mask capped with 3 nm or 6 nm Ru layers. It is suggested that the effect of suppression in the EUV radiation loss associated with Ru etching is canceled by absorption rise, due to the overall oxygen concentration increase.

## **V. ACKNOWLEDGMENTS**

The authors acknowledge the contribution of Peter A. Coon and Gregory Perkins (formerly Intel Corp.) for their help with high resolution XPS analysis; Erik Gullikson (CXRO, LBNL) for his help with reflectivity measurements. This work is funded by Intel Corp., and supported by the Director, Office of Science, Office of Basic Energy Sciences, Division of Materials Sciences and Engineering of the U.S. Department of Energy under Contract No. DE-AC02-05CH11231,

## VI. REFERENCES

- <sup>1</sup> T. E. Madey, N. S. Faradzhev, B. V. Yakshinskiy, and N. V. Edwards, *Appl. Surf. Sci.* **253** (4), 1691 (2006); S. A. Bajt, H. N. Chapman, N. Nguyen, J. Alameda, J. C. Robinson, M. Malinowski, E. Gullikson, A. Aquila, C. Tarrio, and S. Grantham, *Appl. Opt.* **42** (28), 5750 (2003).
- <sup>2</sup> T. Liang, E. Ultanir, G. Zhang, S. J. Park, E. Anderson, E. Gullikson, P. Naulleau, F. Salmassi, P. Mirkarimi, E. Spiller, and S. Baker, *J. Vac. Sci. Technol. B* **25** (6), 2098 (2007).
- <sup>3</sup> W. Kern, *Handbook of Semiconductor Wafer Cleaning Technology - Science, Technology, and Applications*. (William Andrew Publishing/Noyes, 1993).
- <sup>4</sup> F. De Smedt, S. De Gendt, M. Claes, M. M. Heyns, H. Vankerckhoven, and C. Vinckier, *Ozone-Science & Engineering* **24** (5), 379 (2002).
- <sup>5</sup> C. C. Hsu, J. W. Coburn, and D. B. Graves, *J. Vac. Sci. Technol. A* **24** (1), 1 (2006).
- <sup>6</sup> Y. B. He, A. Goriachko, C. Korte, A. Farkas, G. Mellau, P. Dudin, L. Gregoratti, A. Barinov, M. Kiskinova, A. Stierle, N. Kasper, S. Bajt, and H. Over, *J. Phys. Chem. C* **111** (29), 10988 (2007).
- <sup>7</sup> S. Bajt, Z. R. Dai, E. J. Nelson, M. A. Wall, J. B. Alameda, N. Q. Nguyen, S. L. Baker, J. C. Robinson, J. S. Taylor, A. Aquila, and N. V. Edwards, *J. Microlith., Microfab., Microsyst.* **5** (2) (2006).
- <sup>8</sup> H. Over and M. Muhler, *Prog. Surf. Sci.* **72** (1-4), 3 (2003).
- <sup>9</sup> Y. J. Kim, Y. Gao, and S. A. Chambers, *Appl. Surf. Sci.* **120** (3-4), 250 (1997); P. A. Cox, J. B. Goodenough, P. J. Tavener, D. Telles, and R. G. Egdell, *J. Solid State Chem.* **62** (3), 360 (1986).
- <sup>10</sup> H. Over, M. Knapp, E. Lundgren, A. P. Seitsonen, M. Schmid, and P. Varga., *ChemPhysChem* **5** (2), 167 (2004).
- <sup>11</sup> G. A. Somorjai, R. L. York, D. Butcher, and J. Y. Park, *Phys. Chem. Chem. Phys.* **9** (27), 3500 (2007).
- <sup>12</sup> J. Y. Shen, A. Adnot, and S. Kaliaguine, *Appl. Surf. Sci.* **51** (1-2), 47 (1991).
- <sup>13</sup> A. D. Smigelskas and E. O. Kirkendall, *Transactions of the American Institute of Mining and Metallurgical Engineers* **171**, 130 (1947).
- <sup>14</sup> A. Cabot, V. F. Puentes, E. Shevchenko, Y. Yin, L. Balcells, M. A. Marcus, S. M. Hughes, and A. P. Alivisatos, *J. Am. Chem. Soc.* **129** (34), 10358 (2007); Y. D. Yin, R. M. Rioux, C. K. Erdonmez, S. Hughes, G. A. Somorjai, and A. P. Alivisatos, *Science* **304** (5671), 711 (2004).
- <sup>15</sup> E. Lundgren, G. Kresse, C. Klein, M. Borg, J. N. Andersen, M. De Santis, Y. Gauthier, C. Konvicka, M. Schmid, and P. Varga, *Phys. Rev. Lett.* **88** (24) (2002); C. I. Carlisle, T. Fujimoto, W. S. Sim, and D. A. King, *Surf. Sci.* **470** (1-2), 15 (2000).

## VII. FIGURE CAPTIONS AND TABLES

**Figure 1.** High resolution XPS spectra of a 6 nm Ru capping layer on the EUV mask before and after 5 min of oxygen plasma exposure. (a) XPS spectra in the Ru 3d and (b) O1s regions obtained at the normal photoelectron takeoff angle. Solid and broken lines correspond to the sample after oxygen plasma treatment and an untreated sample, respectively. (c) XPS spectra in the Ru 3d and (d) O1s regions obtained at the takeoff angle of  $10^\circ$ .

**Figure 2.** High resolution XPS spectra of a 6 nm and 3 nm Ru capping layer on the EUV mask after 5 min of oxygen plasma exposure. (a) XPS spectra in the Ru 3d<sub>5/2</sub> and (b) O1s obtained at the normal photoelectron takeoff angle. (c) XPS spectra in the Ru 3d<sub>5/2</sub> and (d) O1s obtained at the takeoff angle of  $10^\circ$ . Solid and broken lines correspond to 3 nm and 6 nm Ru capping layers, respectively.

**Figure 3.** The plot of surface roughness ( $\sigma_{\text{RMS}}$ ) of the EUV mask measured with AFM as a function of the oxygen plasma dose.

**Figure 4.** Cross sectional TEM micrographs of the EUV mask top section capped with a 6 nm Ru layer before (a) and after (b) 6 min of oxygen plasma treatment.

**Table I.** The list of Ru 3d and O 1s spectral components used in deconvolution analysis of XPS spectra.

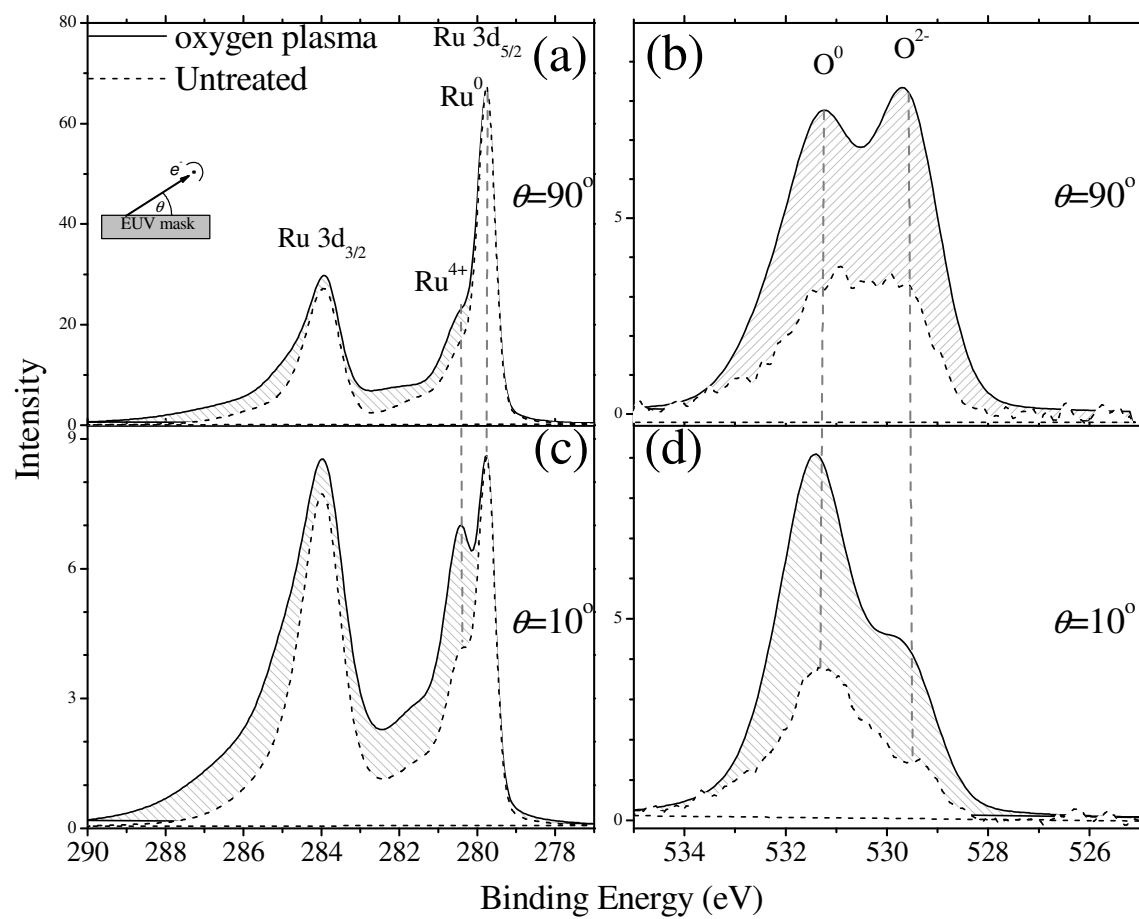


Figure 1.

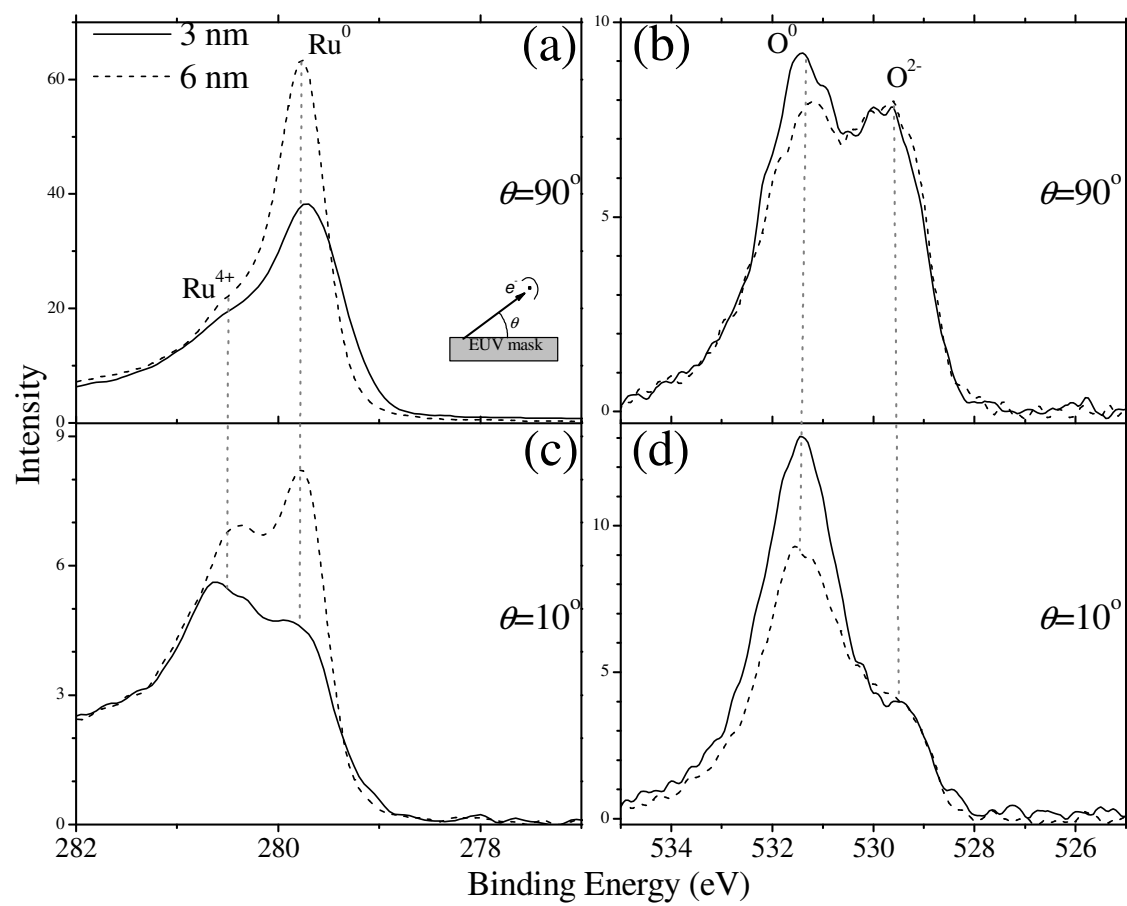


Figure 2.

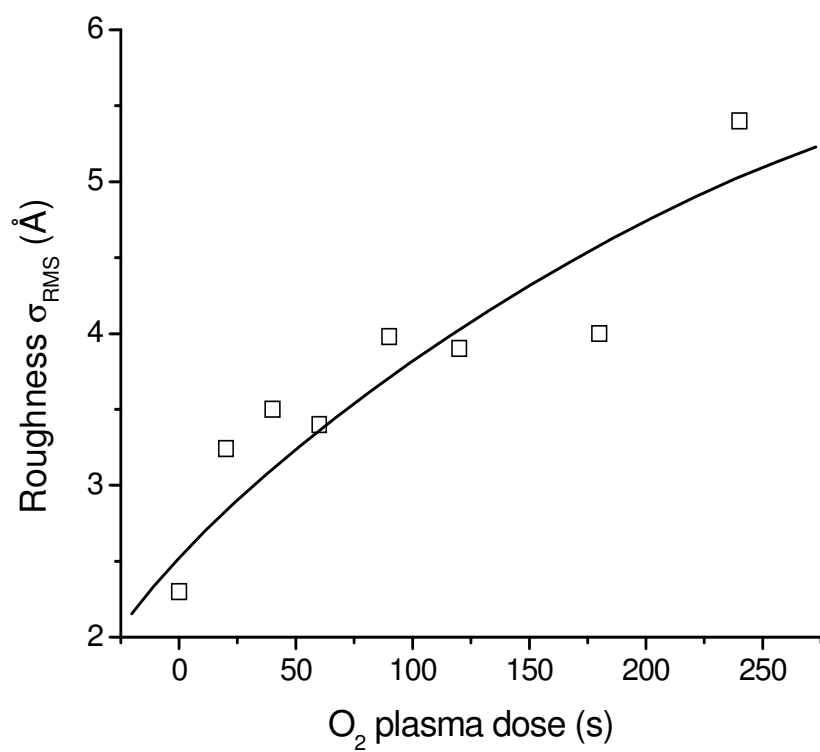


Figure 3.

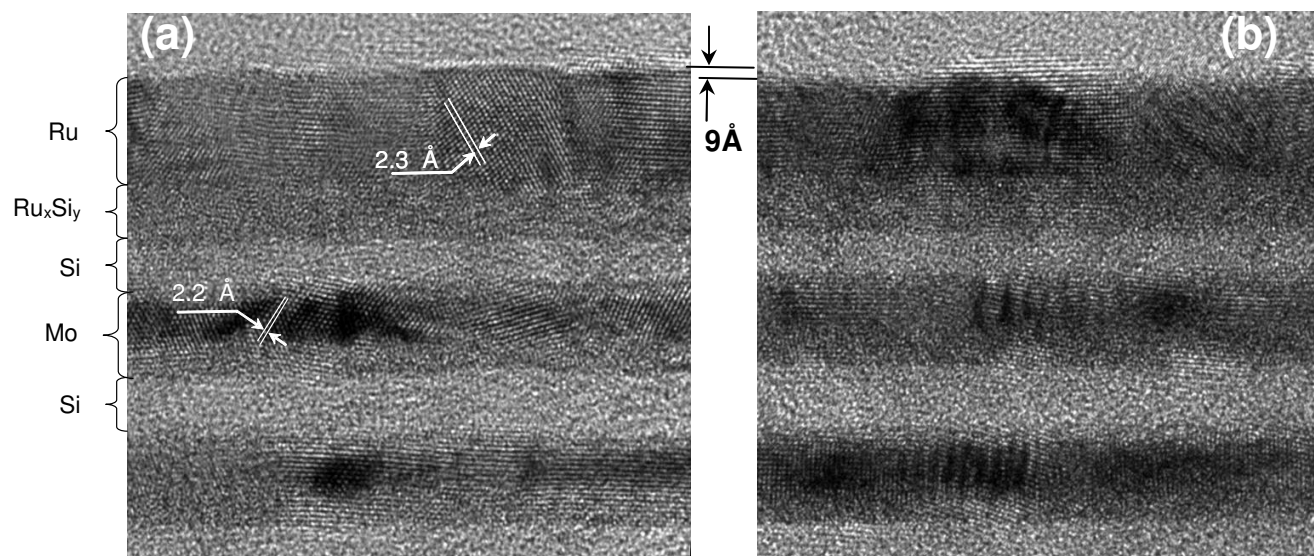


Figure 4.

Table I.

Orbital	Binding Energy (eV)	Oxidation state	Assignment
Ru 3d <sub>5/2</sub>	279.74	0	Metallic Ru
	280.40	4+	<b>RuO<sub>2</sub></b>
Ru 3d <sub>3/2</sub>	283.89	0	Metallic Ru
	284.39	4+	<b>RuO<sub>2</sub></b>
O 1s	531.3	0	Subsurface and chemisorbed
	529.5	2-	<b>RuO<sub>2</sub></b>
C 1s	284.5	0	Organic contamination